ingegneria sismica
International Journal of Earthquake Engineering
Anno XLIII - Num. 1 - 2026

The concept of virtual-real synergy: research on the strategy of building an intelligent digital training platform for higher vocational environmental art design majors

Ling Zhou[1,*] *and Rongliang Wu*[1]

[1] School of Landscape Engineering, Suzhou Polytechnic Institute of Agriculture, Suzhou, Jiangsu, 215008, China

SUMMARY: *This study addresses the issue of suboptimal intelligent effects in the field of environmental art design at vocational colleges. Under the concept of virtual collaboration, it proposes an environmental art design system platform that achieves faster detection efficiency and higher accuracy in object collision detection. A hybrid collision detection technique combining bounding boxes with the fruit fly optimization algorithm is employed. Through iterative fruit fly optimization algorithm calculations, the minimum feature distance is selected. A hybrid collision detection algorithm combining bounding boxes and TCO-FOA is then used to conduct collision detection experiments in virtual scenes. Finally, 62 students from Class 2 of the Environmental Art Design program at a vocational high school in Zhejiang Province were selected as the research subjects. The students' grades followed a normal distribution, with an average score of (64.57 ± 1.24). This method effectively enhances students' interest, attitude, and academic performance in environmental art design courses.*

KEYWORDS: *environmental art design; fruit fly optimization algorithm; bounding box; digital training platform*

1 Introduction

With the rapid development of China's economic construction and the continuous improvement of people's living standards, people have begun to place higher spiritual demands on the artistic quality of their living environment, seeking a more perfect living environment [1-3]. In this social context, the vocational education program in environmental art design has quietly emerged and is gradually developing into an independent discipline. With its broad scope and inherent principles, it aligns with societal needs and has garnered increasing attention [4-7].

Environmental art design is an emerging, interdisciplinary, comprehensive art system engineering field, encompassing multiple disciplines such as fine arts, sculpture, decorative culture, architectural fundamentals, landscape art, ergonomics, design schools, materials science, and psychology [8-11]. It demonstrates significant representativeness both in the breadth of its professional theories and the diversity of its professional skills [12]. Currently, in higher vocational environmental art design programs, schools are continuously increasing investments in laboratory hardware infrastructure, allocating substantial funds. However, challenges persist, including a large number of students, insufficient equipment to meet teaching and training needs, and inadequate training time [13-16]. Therefore, under the digitalization trend, constructing a digital training platform has become a direction for

*m13951824091@163.com
https://doi.org/10.65102/is2026116
Published: 30 April, 2026

improving practical training conditions in higher vocational institutions [17, 18]. The construction of an intelligent platform based on the concept of virtual-physical synergy obtains equipment disassembly processes through on-site video recording, eliminating the need for virtual simulation or animation creation. This approach reduces construction costs, saves time, and enhances realism, thereby effectively assisting in improving the practical skills of vocational college environmental art design students [19-22]. The digital training platform integrates virtual and physical elements in training content, utilizing only images of training room equipment [23, 24]. After the platform is established, teachers can access laboratory equipment in the classroom and select different components based on course requirements, eliminating the need to accompany students to the laboratory. This addresses the inconvenience of using laboratory components for theoretical instruction [25-28]. By leveraging the platform's animation and video resources in conjunction with physical objects, static equipment is dynamicized, compensating for the limitations of static laboratory equipment. This enables students to more easily grasp equipment structure and principles [29-31].

The study first established an intelligent system platform for environmental art design under the backdrop of big data informatization. Under the concept of virtual-physical synergy, the overall framework of the system was developed, and the collision detection technology and the implementation principles of the bounding sphere were introduced. Based on the fruit fly optimization algorithm, a hybrid collision detection algorithm combining bounding box and TCO-FOA was proposed. Additionally, the collision detection functions of the algorithm in this paper were compared with those of other algorithms. Finally, a questionnaire survey was conducted with 62 students from Class 2 of the Environmental Art Design program at a vocational high school in Zhejiang Province as the research case. Teaching practices were conducted in the classroom, and SPSS software was used to analyze the students' learning outcomes, thereby validating the effectiveness of the proposed method.

2 Intelligent construction of a digital training platform based on the concept of virtual-physical synergy

2.1 Construction Concept of Digital Training Platform

Based on the actual teaching practices of general education courses and specialized courses for students, this paper proposes a digital training platform based on the internet, as shown in Figure 1, with the teaching model and process of higher vocational environmental art design as its core. The construction approach is as follows: Utilizing advanced digital technologies, we explore warehouse construction, experience center construction, and visualization of training laboratories to enhance the management of teaching resources, training laboratories, and equipment. We strive to achieve a platform with reasonable hardware, advanced software, and complete functionality, integrating teaching, research, skill practice, school-enterprise cooperation, and social training into a “five-in-one” composite function. This forms a modern engineering training center where teaching, research, and production are organically combined, mutually promoting, and developing together.

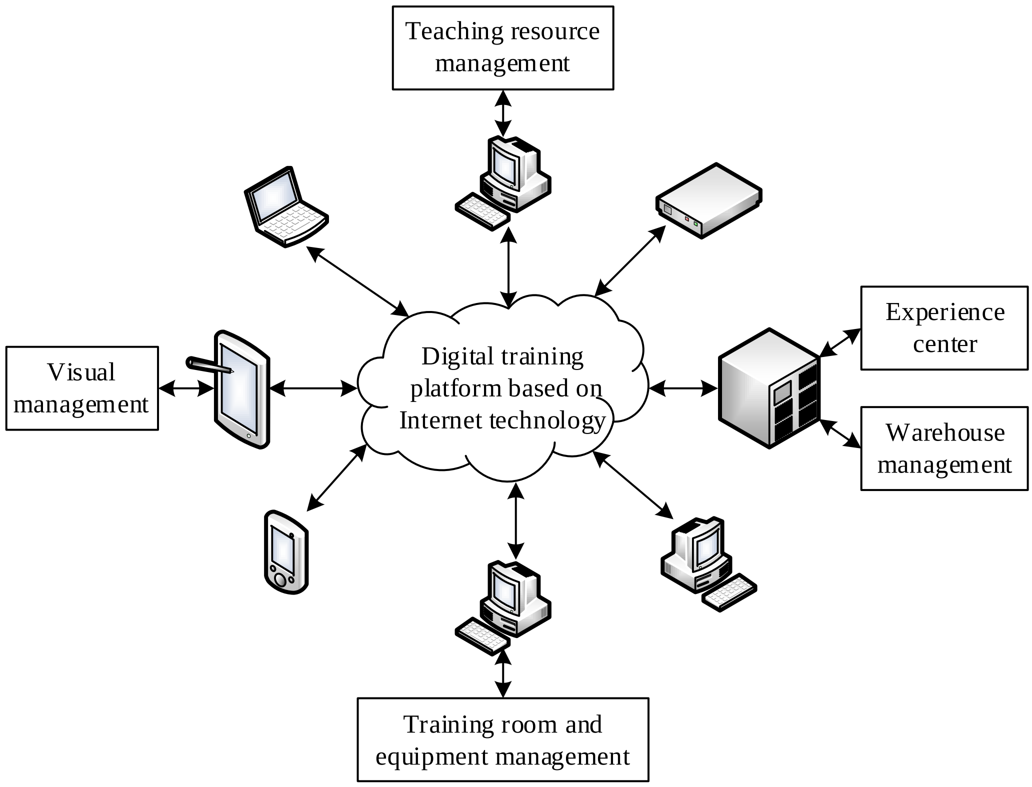

Figure 1: Digital training platform

2.1.1 Warehouse Construction

The Engineering Training Center is the largest on-campus practical training platform in universities. As it undertakes the engineering practical training tasks for the entire university, thousands of students participate in engineering practice at the Engineering Training Center each year, and the daily demand for various consumables and tools is countless. The workload and difficulty of warehouse management at the Engineering Training Center are increasing day by day. Therefore, the construction of an information-based warehouse management system is urgent and meaningful.

2.1.2 Visualization of training rooms

The use of internet technology and wireless video technology to enhance the visualization of training laboratories is a key component of digital training platform construction. This primarily includes the development of a visualization learning platform, internal visualization of training laboratories, and the visualization of the large screen in the engineering training center lobby.

By constructing modules such as machine tool queries in the environmental art design workshop, resource information queries, student growth queries, and introductions to digital workshops, a visualization learning platform can be established that enables self-directed learning and practical training through the internet and various mobile devices. This platform allows both teachers and students to engage in self-directed learning and develop practical skills.

2.1.3 Teaching Resource Management

The teaching resource management platform ensures the advanced nature of practical training content, fully reflecting the production processes and technological development trends of modern enterprises, while also meeting the requirements for expanding practical training capacity and effectively utilizing existing equipment resources. It enables tiered practical training, building on foundational skill training to conduct comprehensive, design-oriented, and innovative high-level training, as well as vocational skill training in areas such as two-dimensional and three-dimensional CAD/CAM numerical control process engineering. It not only facilitates the cultivation of a high-quality training teaching faculty but also stimulates students' interest in learning practical knowledge and improving practical skills, thereby continuously enhancing the quality of training instruction and talent cultivation.

2.2 Digital Training Platform for Environmental Art Design Majors

2.2.1 Geographic Information System

The basic structure of the intelligent environmental technology system platform in the context of big data informatization is shown in Figure 2.

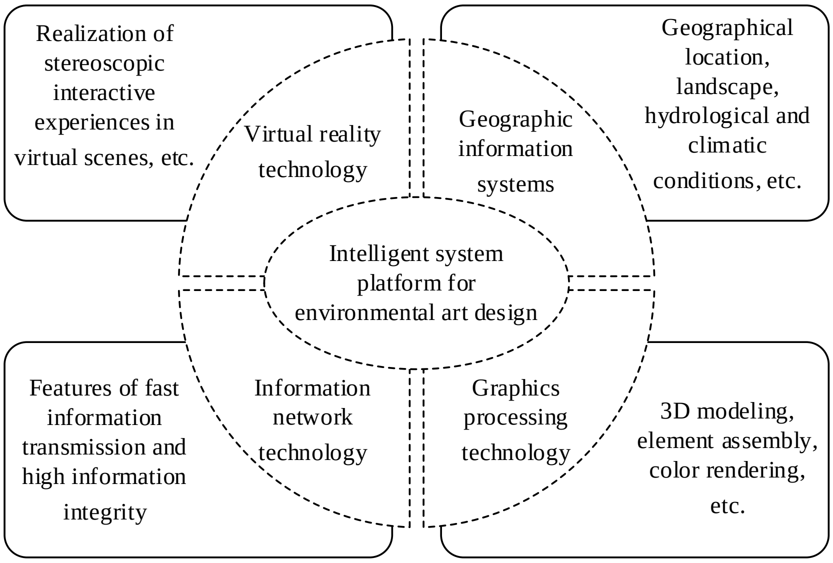

Figure 2: The components of intelligent system platform for environmental art design

Design aspects such as appearance, structure, and form are key factors that environmental art design must focus on. Conducting comprehensive geological surveys and investigations of the surrounding environment is also an important step in ensuring the scientific and rational nature of the design, thereby guaranteeing the scientific, rational, aesthetic, and practical performance of environmental art design.

2.2.2 Graphics processing technology

As an important technical tool in environmental art design, graphic processing technology not only improves the efficiency of environmental art design but also lays the foundation for ensuring the effectiveness of environmental art design. In addition, the application of graphic processing technology in the environmental art design process has significantly enhanced and improved design accuracy, strengthened graphic rendering effects, and provided designers with more design materials. This has not only elevated design standards but also driven environmental art design toward a more diversified and innovative development trend.

2.2.3 Information Network Technology

In the context of the big data and information technology era, the intelligence of environmental art design is primarily manifested in the deep integration of the design process with information networks. Through the continuous integration and development of these two elements, environmental art design is provided with more tools and methods. During the design process, the rapid transmission of information and the realization of synchronous sharing demonstrate the efficiency of network transmission. This also addresses issues such as slow information transmission speeds and information damage in traditional network environments, laying the foundation for improving design quality and effectiveness.

2.2.4 Virtual Reality Technology

In environmental art design, the continuous development of artificial intelligence technology has promoted the application of virtual reality technology. First, the effectiveness of this application is reflected in the presentation of design outcomes. Compared to traditional methods of presenting design outcomes, virtual reality technology can present environmental art design schemes in a more comprehensive and realistic manner to viewers, immersing them in virtual spatial scenarios and enabling interactive experiences that directly stimulate their senses. Secondly, virtual reality technology can also reduce design costs. By leveraging the functionalities of virtual reality technology, designers can minimize cost overruns across various levels in traditional environmental art design, enabling them to better control expenses related to structure, materials, and other aspects, thereby achieving precise cost management in the design process.

3 Intelligent system for environmental optimization design based on FOA

3.1 Basic Principles of Collision Detection

In the basic principles of collision detection, consider two objects A and B in a multidimensional space within an environmental art design scenario. For A object, $a_i \in A(1 \le i \le n)$; simultaneously, for the B object, $b_i \in B(1 \le i \le n)$. Here, n represents the total number of dimensions. The parameters a_i and b_i represent the i th-dimensional features of object A and object B, respectively. The condition for determining whether objects A and B will collide is that the minimum value of the feature distance in the set $F(p)$ is less than the collision detection threshold. In the virtual reality scene of environmental art design, the velocity set of objects A and B is denoted as V and described using formula (1):

$$V = \{V_a, V_b\} = \{(v_{ax}, v_{ay}, v_{az}), (v_{bx}, v_{by}, v_{bz})\} \tag{1}$$

In the equation, v_{ax}, v_{ay}, v_{az} represent the velocities of object A in different directions, respectively, while v_{bx}, v_{by}, v_{bz} represent the velocities of object B in different directions, respectively.

3.2 Bounding Box Technology

There are many types of bounding box techniques, and some classic methods include bounding spheres, axial bounding box (AABB), and oriented bounding box (OBB). Here, we will mainly introduce the basic principles of bounding spheres.

An enveloping sphere is a type of bounding box that is relatively simple to construct but has poor compactness. As an outer sphere of a geometric object, it can create excessive redundant space for objects with many concave surfaces, leading to collisions where the object is not hit but the bounding sphere is instead [32]. To facilitate the explanation of its construction process, we assume here that the geometric object is E, and denote the set of all basic geometric elements (such as triangles and circles) in this object as S_E. The calculation of the bounding sphere is relatively simple compared to other bounding boxes: the average of the three coordinate values of all elements in the set S_E (for triangles, the coordinates of the intersection points of the angle bisectors; for circles, the coordinates of the center) is the center of the bounding sphere, denoted as $c(x, y, z)$. Then, compare the distance from the center of the sphere to each basic geometric element in the object E; the maximum value obtained is the radius of the bounding sphere, denoted as R. As can be seen, the parameters required to record a bounding sphere are much fewer than those for other bounding boxes; obtaining a sphere only requires specifying its center coordinates and radius.

The intersection test method between bounding spheres is also relatively simple, requiring only a comparison of the distance between the centers of the two spheres and the sum of their radii. The specific method is as follows:

Let the centers and radii of the two bounding spheres be: $s_1(x_1, y_1, z_1)$ and R_1 and $s_2(x_2, y_2, z_2)$ and R_2. If $\|s1 - s2\|_2 \le R1 + R2$, then the two bounding spheres intersect; otherwise, they do not intersect. The detailed expression of this inequality is:

$$(x1 - x2)^2 + (y1 - y2)^2 + (z1 - z2)^2 \le (R1 + R2)^2 \tag{2}$$

Since the parameters describing the properties of a sphere remain unchanged regardless of the direction of rotation, the enclosed geometric object will not move outside the bounding sphere no matter how it rotates. Therefore, for an object with a fixed shape, when it moves, the bounding sphere does not need to recalculate its radius; instead, it only needs to translate its center coordinates accordingly. However, for an object whose shape is constantly changing, it is necessary to continuously recalculate the center and radius of the bounding sphere. Therefore, the real-time performance and continuity of the bounding sphere collision detection algorithm are relatively poor.

3.3 Collision Detection in the Fruit Fly Optimization Algorithm

3.3.1 Fruit Fly Optimization Algorithm

The Fruit Fly Optimization Algorithm (FOA) is an optimization algorithm based on the foraging behavior of fruit flies. It leverages the fruit fly's sensitive visual and olfactory characteristics to locate target sources. The FOA algorithm simulates the behavior of fruit flies during the food-seeking process, enabling iterative optimization within a spatial domain [33]. The principle of the FOA algorithm is simple and straightforward, and it is relatively easy to learn. By simulating the olfactory and visual characteristics of fruit flies during their search for food, the solution space is divided into multiple virtual food sources. Each food source represents a solution, while the fruit fly serves as the search agent for the problem. During the search process, the fruit fly selects based on factors such as the quality and distance of the food sources and improves its fitness through local search.

3.3.2 Fruit Fly Algorithm Process

Fruit flies use their keen sense of smell to quickly locate food. Once they are close to their target, they use their vision to locate the food source and other fruit flies. The following is the FOA process:

(1) Assign a value to the maximum number of iterations (Maxgen), $Maxgen = 100$.

(2) The fruit fly's birth position is X_{axis} and Y_{axis} (random positions), where $Rand$ is a random number representing the fruit fly's search step size. The fruit fly then randomly searches for food and regenerates a new position as shown in equation (3).

$$\begin{cases} X(i) = X_{axis} + Rand \\ Y(i) = Y_{axis} + Rand \end{cases} \tag{3}$$

(3) $d(i)$ represents the distance currently traveled by the fruit fly, as shown in equation (4), and $S(i)$ represents the odor concentration value, as shown in equation (5).

$$d(i) = \sqrt{Xi^2 + Yi^2} \tag{4}$$

$$S(i) = 1/d(i) \tag{5}$$

(4) Calculate the current odor concentration value $Smell(i)$ of the fruit fly based on the $S(i)$ value, as shown in Equation (6).

$$Smell(i) = Function(S(i)) \tag{6}$$

(5) Find the individual with the optimal concentration according to equation (7), where $SmellBest$ is the optimal concentration and $IndexBest$ is the optimal fruit fly index.

$$[SmellBest\ IndexBest] = Min(Smell(i)) \tag{7}$$

(6) All individuals fly toward the optimal individual, as shown in Equations (8) and (9).

$$\begin{cases} X_{axis} = X(IndexBest) \\ Y_{axis} = Y(IndexBest) \end{cases} \tag{8}$$

$$SmellBest = BestSmell \tag{9}$$

(7) Repeat steps (2) to (5) until $SmellBest_i < SmellBest_{i-1}$, then execute step 6 to obtain the optimal solution.

3.3.3 Improvements to the Fruit Fly Optimization Algorithm

In the early stages of the fruit fly algorithm iteration, the random step size generated by the upper half-Cauchy distribution can be used to ensure that the step size in the initial stage is small and relatively uniform. As the iteration progresses, the step size gradually increases, exhibiting an S-shaped growth trend. This setting helps the fruit fly optimization algorithm to explore more in the early stages of iteration and utilize the excellent solutions discovered in the later stages of iteration.

The ascending half-Cauchy distribution function is given by Equation (10).

$$f(x)=\begin{cases}0, x\le a\\ \dfrac{1}{1+b(x-a)^{-1}}, x>a(b,c>0)\end{cases} \tag{10}$$

In Equation (10), $a=0.2$, $b=50$, and $c=2$. When $x\le a$, the step size is small and relatively uniform, making it less likely to lose the optimal solution during the search process. When $x>a$, the search step size gradually increases to expand the search range. When approaching 1, the convergence speed of the search step size accelerates to achieve a more effective search strategy.

Additionally, the fruit fly optimization algorithm can introduce randomness based on the characteristics of the Cauchy distribution, making the step size more variable, thereby enhancing both global exploration capabilities and local optimization capabilities during the search process. The Cauchy distribution function is given by Equation (11).

$$F(x)=\frac{1}{2}+\frac{1}{\pi}*\arctan x, -\infty<x<+\infty \tag{11}$$

This study proposes a new mutation operation method—the Cauchy mutation factor—based on the characteristics of the Cauchy distribution, to replace the traditional exponential function. By utilizing random numbers generated from the Cauchy distribution, the Cauchy mutation factor is more likely to produce values far from the origin, resulting in a more pronounced change trend compared to the exponential function. This is particularly helpful for the fruit fly optimization algorithm to escape local optima during the iteration process. The functional equation of the Cauchy mutation factor is given by Equation (12).

$$Z=\exp\Big(\tan\big(\big(rand(-1,1)-1/2\big)\pi\big)\Big) \tag{12}$$

This study improved the FOA algorithm to obtain the TCO-FOA algorithm, which is an algorithm that changes the search step length of fruit flies based on the rate of change in the average concentration. The improvement process is as follows.

First, the average concentration change ratio A_{Rate} is calculated using Equations (13) to (15).

$$Avg(i)=\frac{\max(Smell(i))+\min(Smell(i))}{2} \tag{13}$$

$$Avg(i-1)=\frac{\max(Smell(i-1))+\min(Smell(i-1))}{2} \tag{14}$$

$$A_{Rate}=\frac{Avg(i)}{Avg(i-1)} \tag{15}$$

Then, improve the growth rate using the calculated A_{Rate}, as shown in equation (16).

$$L_i = \begin{cases} L_{i-1} + \exp\left(A\left(\dfrac{m-1}{Maxgen} \right) \right) + K, & A_{Rate} > 1 \\ L_{i-1} - \exp\left(\tan(1 - A_{Rate}) \right) * \dfrac{m-1}{Maxgen} * Z - K, & A_{Rate} \leqslant 1 \end{cases} \tag{16}$$

Then, equation (3) can be optimized to equation (17).

$$\begin{cases} X(i) = X_{axis} + L_{i-1} * Rand \\ Y(i) = Y_{axis} + L_{i-1} * Rand \end{cases} \tag{17}$$

In Equations (13) to (17), L_i and L_{i-1} represent the current iteration search step size and the previous iteration search step size of the fruit fly, respectively, A_{Rate} represents the average concentration change rate, and m represents the number of iterations in the fruit fly optimization algorithm. Z is the Cauchy mutation factor, and K is the dynamic compensation factor. Experimental analysis indicates that the optimal value for $K = 1.5$.

3.3.4 Inspection Process

First, select the bounding box type based on the shape of the virtual object; then determine whether the objects have collided based on whether there is overlap between the bounding boxes. If there is overlapping space between the bounding boxes, a collision occurs, and the second step is executed; then, based on the extracted two-dimensional coordinates, a fruit fly population is constructed, with the population size and maximum iteration count set. The objective function is the feature distance $F(P)$ between the objects to be detected, and $F(P)$ is compared with the collision threshold δ to determine whether a collision has occurred. If the similarity distance $F(P)$ between the objects to be detected is less than the collision threshold δ, it can be determined that the objects have collided; otherwise, it is considered that they have not collided. The collision threshold δ is a dynamic value. First, based on research and literature in related fields, understand the threshold settings used in similar problems as a reference point for the initial threshold; then verify its effectiveness through actual experiments and tests and adjust its size accordingly.

3.4 Example Simulation

To validate the performance of the fruit fly optimization algorithm in virtual reality collision detection, instance simulations were conducted using the MATLAB 2018b simulation platform. The simulation data was sourced from a 3D animated film produced by an animation company, with an animation scene boundary of 100 cm × 100 cm × 80 cm cube and a total of 86 character objects.

3.4.1 Impact of Key Parameters on Collision Detection Performance

Differentiate the number of object features selected in the enclosed intersecting space. The number of samples selected is 1000, forming feature pairs with dimensions of 100×100, 3000 × 300, 500 × 500, and 700 × 700, respectively. The upper and lower limits of the fruit fly odor concentration change rate (Rmax and Rmin) were set differently, and the collision detection accuracy rates are shown in Tables 1–4. Comparing Tables 1–4, it can be seen that under the same number of feature pairs, the upper and lower limits of the odor concentration change rate

R significantly affect the collision detection accuracy in virtual reality. The experiments indicate that regardless of the number of feature pairs selected in the detection samples, the upper and lower limit settings of R significantly impact the collision detection performance of the improved FOA algorithm.

When comparing different feature pair counts, when the sampled feature pair count is 100×100, R achieves the highest detection accuracy of 0.8493 within the range [0.8, 1.2]; When the number of sampled feature pairs is 300×300, R achieves the highest detection accuracy of 0.8858 within the range [0.9, 1.2]; When the number of sampled feature pairs is 500×500, R achieves the highest detection accuracy of 0.9457 within the range [1.0, 1.2]; When the number of sampled features is 700×700, R achieves the highest detection accuracy of 0.9589 within the range [0.9, 1.2]. Therefore, the highest collision detection rates vary significantly for different numbers of sampled features, and the more object features sampled, the better the collision detection performance of the bounding box + TCO-FOA.

*Table 1: Detection accuracy of different r values (logistic regression 100*100)*

R_{min}	R_{max}			
	1.1	1.2	1.3	1.4
0.7	0.7811	0.8311	0.8114	0.7742
0.8	0.8189	**0.8493**	0.8132	0.7882
0.9	0.8273	0.8412	0.8273	0.7976
1.0	0.8325	0.8274	0.8142	0.8091

*Table 2: Detection accuracy of different r values (logistic regression model 300*300)*

R_{min}	R_{max}			
	1.1	1.2	1.3	1.4
0.7	0.8186	0.8672	0.8225	0.7791
0.8	0.8301	0.8722	0.8315	0.8179
0.9	0.8439	**0.8858**	0.8532	0.8274
1.0	0.8545	0.8665	0.8595	0.8413

Table 3: Detection accuracy of different r values (logistic regression 500 500)*

R_{min}	R_{max}			
	1.1	1.2	1.3	1.4
0.7	0.8741	0.8689	0.8629	0.8728
0.8	0.9229	0.8912	0.9263	0.9184
0.9	0.9047	0.9416	0.9372	0.9245
1.0	0.9343	**0.9457**	0.9132	0.9111

*Table 4: Detection accuracy of different r values (Characteristic logarithm 700*700)*

R_{min}	R_{max}			
	1.1	1.2	1.3	1.4
0.7	0.8831	0.9293	0.9195	0.9264
0.8	0.9108	0.9308	0.9305	0.9306
0.9	0.9328	**0.9589**	0.9573	0.9449
1.0	0.9368	0.9461	0.9308	0.9357

3.4.2 Improving the collision detection performance of the fruit fly algorithm

Collision detection was performed on objects within the overlapping regions of 1,000 sample sets. The sampling feature dimensions were 100×100, 300×300, 500×500, and 700×700, respectively. Both bounding box technology and bounding box technology combined with the fruit fly optimization algorithm were used to simulate virtual teaching samples. The simulation results are shown in Figure 3. As the number of sampled feature pairs increases, the detection accuracy of all three algorithms improves. A larger number of features can more accurately reflect the position and motion state of objects, providing more comprehensive data samples for the execution of detection algorithms. As shown in the figure, when the number of feature pairs reaches 700×700, the detection accuracy does not improve significantly compared to 500×500. This indicates that selecting 500 feature pairs is more appropriate, as a larger number of feature pairs inevitably increases collision detection time. When comparing the detection accuracy rates of the three algorithms, the bounding box technique has the lowest accuracy rate, with a maximum value of around 0.85. After undergoing two-stage collision detection using the bounding box and FOA techniques, the detection accuracy rate improves significantly. After the FOA technique is improved, its detection accuracy rate becomes even higher. When the number of feature pairs is 500×500, the accuracy rate improves by 0.23.

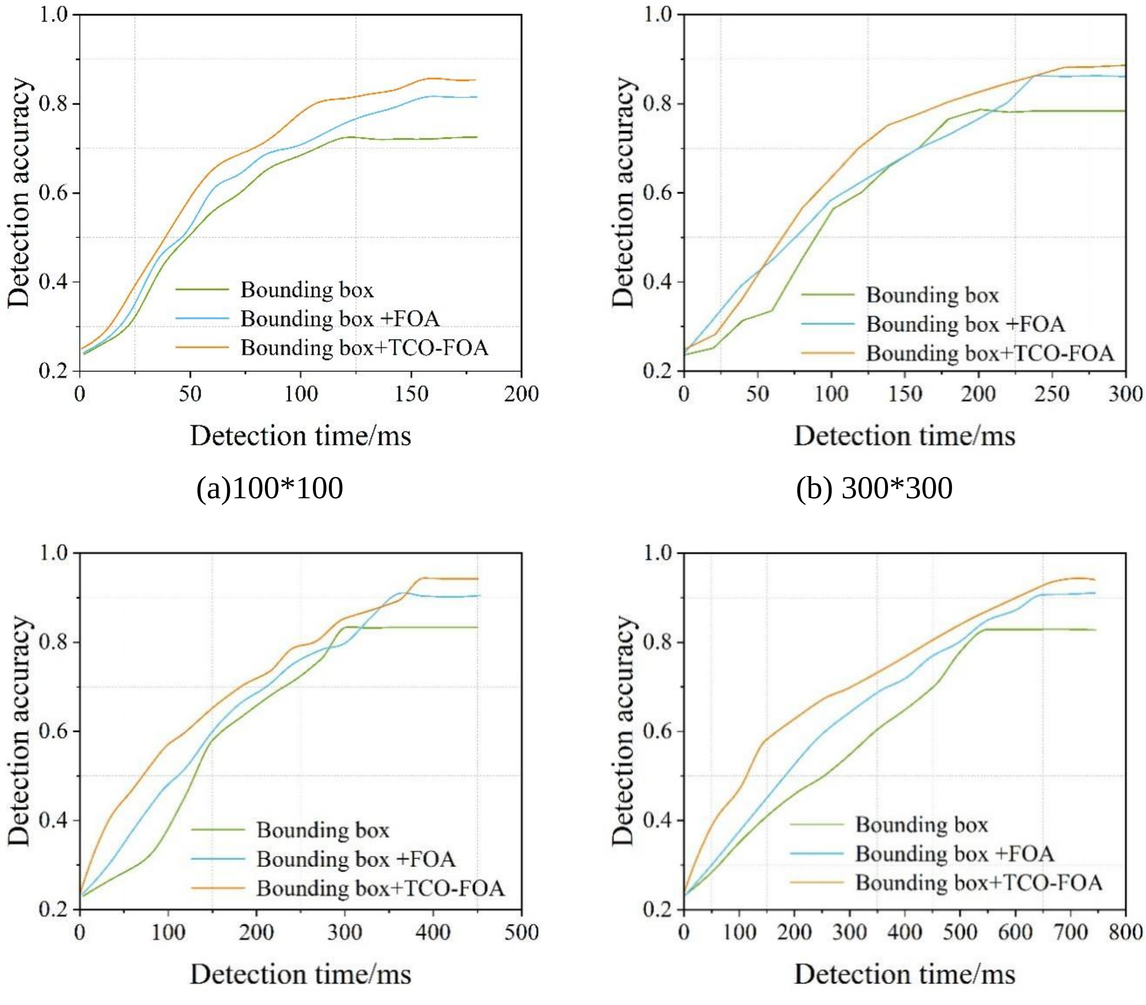

(a)100*100 (b) 300*300

(c)100*100 (d) 300*300

Figure 3: Collision detection performance of the three algorithms

Performance simulations were conducted on the root mean square error (RMSE) of detection accuracy and detection time for the three algorithms, with the statistical results shown in Table 5. As can be seen from the table, as the number of sampled features increases, the RMSE of collision detection accuracy for all three algorithms decreases. This is primarily because a larger number of sampled features facilitates the algorithms' ability to detect collisions along object edges. A comparative analysis of the three algorithms reveals that the bounding box technique combined with the TCO-FOA algorithm achieves the optimal RMSE performance, with an RMSE of only 0.02714 when the feature size is 700×700.

Table 5: Collision detection time and RMSE under different sampling scales

Algorithm	Number of features	RMSE	Detection time/ms
Encircling box technology	100*100	8.113E-02	129.197
	300*300	7.572E-02	196.698
	500*500	6.216E-02	311.725
	700*700	5.693E-02	479.647
Enclosing box technology +FOA	100*100	7.631E-02	150.361
	300*300	5.252E-02	244.236
	500*500	4.413E-02	386.846
	700*700	3.197E-02	631.511
Enclosing box technology+TCO-FOA	100*100	6.471E-02	159.574
	300*300	4.093E-02	260.629
	500*500	3.103E-02	408.169
	700*700	2.714E-02	720.227

4 Practice and Analysis of the Vocational College Environmental Art Design Professional Training Platform

4.1 Practical Cases

Blending Virtual and Real-World Applications: This case study selected 62 students from Class 2 of the Environmental Art Design program at a vocational high school in Zhejiang Province. The students were divided into two groups, with one group using traditional teacher-led instruction and the other using an FOA-based intelligent teaching platform for environmental art design. Initially, the traditional teacher-led instruction was conducted in small groups, followed by individual use of the FOA-based intelligent teaching platform for environmental art design. There are two reasons for this approach. First, it helps students become familiar with the operations of both methods. Second, since this activity marks students' first formal exposure to the intelligent platform and environmental art design, completing the design collaboratively under teacher-led instruction first, followed by individual practice on the intelligent platform, can deepen students' understanding of key and challenging concepts—particularly in environmental art design—helping them clarify their thinking and overcome the challenges of the subject.

The teaching effectiveness questionnaire for applying the FOA-based intelligent teaching platform in environmental art design classrooms is divided into a student learning attitude questionnaire and a learning ability survey questionnaire. After collecting the questionnaires, the data was analyzed using SPSS 21.0.

4.2 Questionnaire Analysis

4.2.1 Analysis of the Learning Attitude Questionnaire

(1) Paired-sample t-test analysis

A paired-sample t-test was conducted on the learning attitude questionnaires completed by students in Class 2 of the Environmental Art Design program. The results are summarized in Table 6. In the table, for the "learning interest" dimension, the mean value of the students in this class before the experiment was 3.51, with a standard deviation of 0.71 and a standard error of 0.09. After more than two months of experimentation, the mean value of learning interest was 4.06, with a standard deviation of 0.45 and a standard error of 0.05. The mean value of the post-test sample was higher than that of the pre-test.

Table 6: Pairwise sample statistics

Dimension	The testing phase	Mean	N	Standard error	Standard error of mean
Learning interest	Before measurement	3.508	62	0.7151	0.0915
	After test	4.063	62	0.4536	0.0509
Attitude to learning	Before measurement	2.977	62	0.3959	0.0532
	After test	3.481	62	0.2978	0.0402
Recognition of learning effectiveness	Before measurement	3.104	62	0.4735	0.0635
	After test	3.979	62	0.3241	0.0437
Recognition of teaching methods	Before measurement	3.022	62	0.6282	0.084
	After test	3.958	62	0.4586	0.0515

Further sample tests were conducted, with the results shown in Table 7. As can be seen from the table, the sig values for all four dimensions of the learning attitude questionnaire were 0.000 < 0.05, indicating a significant positive correlation between the pre- and post-measurement data. This suggests that a t-test can be conducted, with the results shown in Table 8. It can be observed that the mean values for all four dimensions showed varying degrees of improvement, with the dimensions of learning effectiveness recognition and teaching method recognition showing more pronounced improvements. Taking the "learning effectiveness recognition" dimension as an example, the mean difference in students' perceived effectiveness of learning environmental art design courses was 0.8817. The t-value for the mean difference test was 17.116, with df = 62, and the significance level P-value was 0.000 < 0.05, reaching a significant level. This indicates that at the beginning of the teaching practice, students had a relatively high level of interest in learning environmental art design courses.

Table 7: Correlation coefficient of paired samples

Dimension	N	Correlation coefficient	Sig.
Learning interest pre-test & learning interest post-test	62	0.774	0.000
Learning attitude pre-test & learning attitude post-test	62	0.451	0.000
Learning effect recognition pre-test & learning effect recognition post-test	62	0.632	0.000
Pre-test of teaching method recognition and post-test of teaching method recognition	62	0.579	0.000

Table 8: Pairwise sample test

	Chorus differential					t	Df	Sig.
	Mean	Standard error	Standard error of mean	95% confidence interval for the difference				
				lower limit	superior limit			
Learning interest	-0.5521	0.4735	0.0593	-0.6822	-0.4328	-9.275	62	0.000
Learning attitude	-0.5132	0.3814	0.0475	-0.6104	-0.4173	-11.543	62	0.000
Learning effect recognition	-0.8817	0.3729	0.0479	-0.9714	-0.7784	-17.116	62	0.000
Teaching method recognition	-0.9256	0.5273	0.0691	-1.0923	-0.7982	-12.015	62	0.000

(2) Correlation analysis between the "teaching method recognition" dimension and other dimensions

To understand the correlation between the three dimensions of "learning interest," "learning attitude," and "learning effectiveness recognition" in the attitude questionnaire and teaching method recognition, correlation tests were conducted on the post-test data for each of the above dimensions. The results are shown in Figure 4. According to the scatter plot, the "teaching method recognition" dimension shows a strong correlation with the "learning interest" dimension, while its correlation with "learning attitude" and "learning effectiveness recognition" is weaker compared to "learning interest."

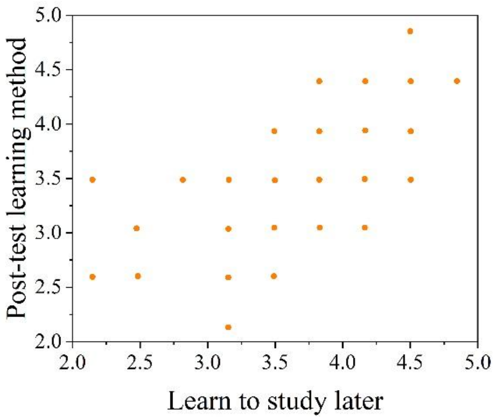

(a) Learning interest

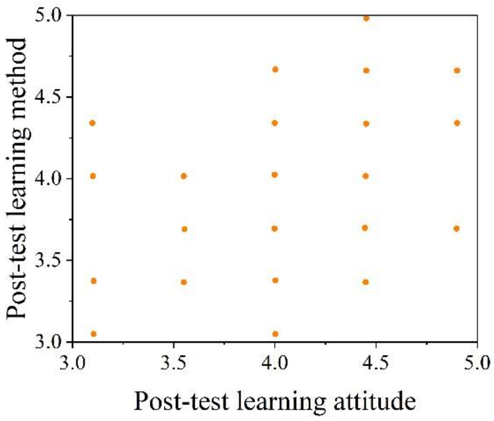

(b) Attitude to learning

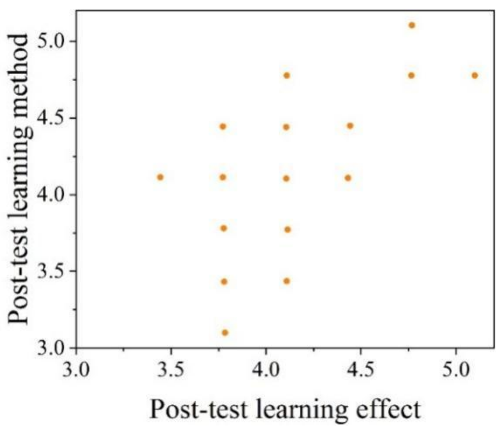

(c) Educational value

Figure 4: correlation scatter plot

The correlation test between the “teaching method recognition” dimension and other dimensions is shown in Table 9. All dimensions of “teaching method recognition” are significantly correlated with Sig. = 0.000 (<0.01). Among them, the correlation with “learning interest” is the strongest, with a correlation coefficient of 0.637. The correlation coefficients with the other two dimensions are 0.627 and 0.563, respectively, and there is also a significant correlation. This indicates that the use of a blended digital training platform significantly improves students' attitudes toward learning environmental art design courses.

Table 9: Correlation test

		Learning interest	Aattitude to learning	Educational value
Recognition of teaching methods	Pearson correlation	0.637**	0.627**	0.563**
	Significance (bilateral)	0.000	0.000	0.000
	The sum of squares and cross products	7.014	5.275	0.079
	Covariance	0.133	0.079	0.081
	N	62	62	62

4.2.2 Analysis of Student Learning Ability Questionnaire

A paired-sample t-test was conducted on the learning ability questionnaires completed by 62 students. The results are summarized in Tables 10 and 11. The data show that after the practical training, students' abilities in the environmental art design course using the FOA-based teaching intelligent platform environment were significantly different in terms of knowledge level, logical thinking, and innovative ability, with p-values all less than 0.05. This indicates that there are significant differences between the data, and a paired-sample t-test can be performed. As shown in the table data, after completing the environmental art design professional course, students' knowledge levels and logical thinking abilities in environmental art design have significantly improved, with mean differences of 1.32 points and 0.76, respectively. This indicates that the use of a blended learning approach (combining virtual and physical elements) is beneficial for enhancing students' knowledge levels and fostering the development of logical thinking skills.

Table 10: Pairwise sample test

Dimension	The testing phase	Mean	Mean difference	Standard deviation	Standard error of mean	t	Sig.
Knowledge Level	Before measurement	2.7932	1.3204	0.51282	0.07143	24.092	0.000
	After test	4.1136		0.31251	0.05125		
Logical thinking	Before measurement	3.0721	0.7601	0.41128	0.06208	16.114	0.000
	After test	3.8322		0.32572	0.05074		
Innovation ability	Before measurement	3.0457	0.3006	0.47186	0.05974	8.943	0.000
	After test	3.3463		0.44742	0.05471		

Table 11: Sample correlation coefficient

Dimension	N	Correlation	Sig.
Knowledge level pre-test & knowledge level post-test	62	0.772	0.000
Logical thinking pre-test & logical thinking post-test	62	0.451	0.000
Innovation ability pre-test & innovation ability post-test	62	0.629	0.000

4.3 Test Score Analysis

The distribution of final exam scores is shown in Figure 5. SPSS 21.0 software was used to analyze the students' test scores. There were 62 students who took the exam, with 57 valid scores. The total score was 100 points, and the pass rate was 62.1%. The analysis in SPSS showed that the students' scores in this exam were basically normally distributed, with a mean of 64.57 and a standard deviation of 11.24.

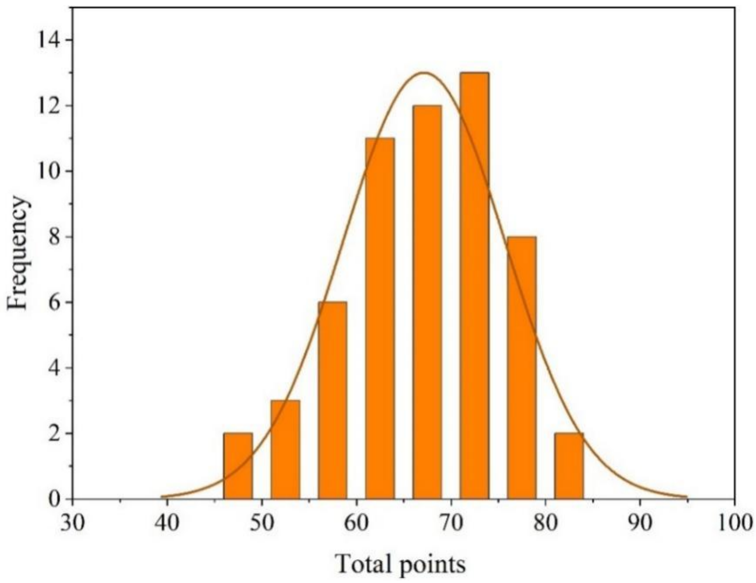

Figure 5: Distribution of final exam scores

The test questions are categorized based on the content being assessed, with the questions divided into four sections: “Fundamental Knowledge,” “Spatial Design,” “Architectural Landscape Design,” and “Software Operation.” The students' scores for each section are shown in Table 12. As shown in the table, students performed best in the “Basic Knowledge” section, with an average score of 32.14 (passing score: 28.9), indicating that through practical experience, students have a good grasp of basic knowledge. In terms of “Software Operation,” the average score was 15.18 (passing score: 12.8), with a standard deviation of 3.156, suggesting that students generally performed well in sensor selection and application.

Table 12: Student scores

	N	Minimal	Maxima	Mean	Standard error of mean	Standard error	Variance
Basic Knowledge	62	21	44	32.09	0.866	6.784	42.517
Space design	62	3	11	5.13	5.214	1.972	3.148
Architectural landscape design	62	7	25	13.04	13.09	3.735	14.792
Software operations	62	10	19	15.18	14.97	3.156	10.153
N	62						

5 Conclusion

Based on the fruit fly optimization algorithm, combined with environmental technology in the context of big data informatization, an intelligent training platform for environmental art design was constructed and applied. Through a comparison of different algorithms, the bounding box + TCO-FOA algorithm proposed in this paper effectively improved the collision detection rate of objects in the environmental art design context, with a detection time of 720 ms. Although this is longer than other algorithms, it has the best overall performance. Finally, a case study was selected for practical analysis. In the “learning attitude” dimension, the mean difference between pre- and post-tests was 0.5. According to the mean analysis of the questions, students demonstrated a strong willingness to continue learning. Additionally, the correlation coefficient between learning attitude and teaching method acceptance was 0.627, indicating a moderate correlation. This suggests that the use of a blended learning approach in environmental art design courses can effectively enhance students' learning interest.

Funding

This work was supported by "Dual-Context Coupling and Dual-Integration Promotion": Research on Digital Training Mode for Higher Vocational Environmental Art Design Major (XHYBLX2025222), a 2025-2026 Jiangsu Vocational Education Research Project of Jiangsu Vocational Education Association.

The 2025 educational science planning project of Jiangsu Provincial Academy of Educational Sciences, titled "Research on Strategies for Innovating Talent Cultivation Models in Art and Design Majors Empowered by Artificial Intelligence" (Project No.: C/2025/02/101);

About the Authors

Ling Zhou was born in Jiangsu, P.R. China, in 1993. I obtained a master's degree from Nanjing Forestry University. I am currently working as a dedicated teacher at Suzhou Polytechnic Institute of Agriculture. My main research direction is environmental art design.

Rongliang Wu was born in Henan, P.R. China, in 1989. I obtained a master's degree from Jiangnan University in China. Employed at Suzhou Polytechnic Institute of Agriculture. My main research directions are architectural indoor and outdoor environment design, and vocational education.

References

[1] Chen, Y., Hicks, A., & While, A. E. (2013). Quality of life of older people in China: A systematic review. Reviews in Clinical Gerontology, 23(1), 88-100.

[2] Zou, S., Feng, G., Li, D., Ge, P., Wang, S., Liu, T., ... & Ming, W. K. (2022). Lifestyles and health-related quality of life in Chinese people: a national family study. BMC public health, 22(1), 2208.

[3] Zhang, K. C., & Yu, E. D. (2014). Quest for a good life: spiritual values, life goals, and college students. Asia-Pacific Psychiatry, 6(1).

[4] Kang, J. (2021, April). Innovative research and development of the teaching mode of

environmental art design major in universities. In 2021 2nd Asia-Pacific Conference on Image Processing, Electronics and Computers (pp. 435-439).

[5] Zhao, W. (2016, March). Three forms in one to create higher vocational education art talents training space: Practical exploration on the organic integration of professional form, teaching form, environment form. In 2016 IEEE Symposium on Service-Oriented System Engineering (SOSE) (pp. 293-296). IEEE.

[6] Zhu, J., & Wang, D. (2023). Research on curriculum reform of environmental art and design majors in higher vocational education based on school-enterprise cooperation. Advances in Vocational and Technical Education, 5(8), 6.

[7] Wang, N., Ye, J. H., Gao, W., Lee, Y. S., Zeng, L., & Wang, L. (2024). What do they Need?—The academic counseling needs of students majoring in art and design in a higher vocational college in China. Heliyon, 10(6).

[8] Niu, F. (2021). Communicative image expression in teaching of computer-aided design for environmental art major. Computer-Aided Design & Applications, 18.

[9] Xiong, C. (2022, January). The Application of Computer Three-dimensional Modelling Technology in Environmental Art Design Major. In 2022 3rd International Conference on Education, Knowledge and Information Management (ICEKIM) (pp. 961-964). IEEE.

[10] Kou, Y. (2022). Construction and Application of Curriculum System of Design Major Integrating Environmental Protection and Big Data. Journal of Environmental and Public Health, 2022(1), 7496172.

[11] Dong, C., & Li, X. (2024). Research on Teaching Reform and Practice of Graduate Design for Environmental Design Major Based on OBE Concept under the Background of New Liberal Arts. International Journal of New Developments in Education, 6(7).

[12] Wang, Y. (2024, July). The Integration of Information Technology and Environmental Art Design: Development Path and Value Exploration. In International Conference on Digital Classroom & Smart Learning (pp. 284-293). Cham: Springer Nature Switzerland.

[13] Jokela, T., & Coutts, G. (2018). The North and the Arctic: A laboratory of art and design education for sustainability. Relate North: Art and design education for sustainability, 98-117.

[14] Mingmei, Z. (2024). Research on" 2+ 2+ 1" Environmental Art Design Talent Cultivation Mode. Frontiers in Art Research, 6(4), 060410.

[15] Kaya, N., & Satir, S. (2015). Improving fundamental values and environmental awareness in sustainable engineering education through laboratory and design experiments. Hittite Journal of Science and Engineering, 2(1), 103-114.

[16] Go, I. G. (2022). A study on the design of a practical arts laboratory for elementary level technology education in Korea. EURASIA Journal of Mathematics, Science and Technology Education, 18(6), em2122.

[17] Ye, Y. T. (2016). Design and Implementation of Digital Art Teaching System Based on

Interactive Virtual Technology. International Journal of Emerging Technologies in Learning, 11(11).

[18] Huang, F., & Xu, J. (2024). New Teaching Approaches to Art and Design Education in the Digital Age. In SHS Web of Conferences (Vol. 181, p. 01046). EDP Sciences.

[19] Liu, Y., & Ko, Y. C. (2023). The optimization of digital art teaching platform based on information technology and deep learning. IEEE Access, 11, 107287-107296.

[20] Huang, H. (2025). The cultivation of quality and ability of environmental design professionals in universities under the digital background. International Educational Research, 8(3), p25-p25.

[21] Zhang, C., & Li, X. (2023). Construction of Digital Art Education Platform under the “Internet+” Environment. Mobile Information Systems, 2023(1), 8453791.

[22] Jiecheng, W. (2023). Analyze the application of new media technology in environmental art design. Procedia Computer Science, 228, 907-913.

[23] Huang, Y., Lin, M., & Liu, X. (2024). Digital media and interactive E-learning application in art teaching process based on big data platform. Entertainment Computing, 51, 100737.

[24] Li, D. (2022). Application of Hand-Painted Expression in Environmental Design Teaching. International Journal of New Developments in Education, 4(12).

[25] Agudamu. (2022, October). Application of Virtual Learning Model based on UML Software Design in Art Design Network Platform Design. In 2022 3rd International Conference on Smart Electronics and Communication (ICOSEC) (pp. 1178-1181). IEEE.

[26] Xiaolan, Z., & Ping, G. (2020). Exploration on the Mode of Training Practical Ability of Digital Media Art Major in Application-Oriented Universities. Frontiers in Art Research, 2(9).

[27] Gan, L. (2022). Talking about the application of new media art in environmental art design. International Journal of Education and Teaching Research, 3(3).

[28] Lunevich, L. (2021). Critical digital pedagogy and innovative model, revisiting Plato and Kant: An environmental approach to teaching in the digital era. Creative Education, 12(9), 2011-2024.

[29] Svitlana, P. S. P., & Tetiana, L. T. L. (2023). The impact of digitalization on the art market actors' activity management. Revue scientifique" Ukrainian Journal of Applied Economics and Technology", 8(4), 69-73.

[30] Gong, Y. (2024). Research on the Application of Digital Technology in Environmental Art Design. Journal of Modern Educational Theory and Practice, 1(2).

[31] Jin, H., & Yang, J. (2022). Using computer-aided design software in teaching environmental art design. Computer-Aided Design & Applications, 19.

[32] Huang Xiangyang, Zhang Shudong, Zhou Lijuan & Huang LiGuo. (2022). A hybrid

algorithm for the minimum bounding sphere problem. Operations Research Letters, 50(2), 150-154.

[33] Xiao Zhou, Jun Wang, Wenbing Liu, Fan Jiang & Rui Li. (2025). Intelligent Emergency Logistics Route Model Based on Cellular Space AGNES Clustering and Symmetrical Fruit Fly Optimization Algorithm. Symmetry, 17(5), 649-649.